Inorg. Chem. **2005**, *44*, 1941–1949

DFT Study of Unligated and Ligated Manganese^{II} Porphyrins and Phthalocyanines

Meng-Sheng Liao, John D. Watts, and Ming-Ju Huang*

Department of Chemistry, P.O. Box 17910, Jackson State University, Jackson, Mississippi 39217

Received September 2, 2004

A theoretical study of the electronic structure, bonding, and properties of unligated and ligated manganese^{II} porphyrins and phthalocyanines has been carried out "in detail" using a density functional theory (DFT) method. While manganese tetraphenylporphine (MnTPP) in the crystal is high spin ($S = {}^5/_2$) with the Mn^{II} atom out of the porphyrin plane, the present calculations find that the free manganese porphine (MnP) molecule has no obvious tendency to distort from planarity even in the high-spin state. The ground state of the planar structure is found to be intermediate spin ($S = {}^3/_2$). Manganese phthalocyanine (MnPc) is calculated to have a ^4E_g ground state, in agreement with the more recent magnetic circular dichroism (MCD) and UV–vis measurements of the molecule in an argon matrix but different from the early magnetic measurements of solid MnPc. The effect of the crystal structure on the electronic state of MnPc is examined by the calculations of a model system. For the six-coordinate adducts with two pyridine (py) ligands, the strong-field axial ligands raise the energy of the Mn d_{z^2}-orbital, thereby making the Mn^{II} ion low spin ($S = {}^1/_2$). The recent assignment of $MnPc(py)_2$ as an intermediate-spin state proves to be incorrect. Some issues involved in the reduced products have also been clarified. Five-coordinate MnP(py) and MnPc(py) complexes are high spin and intermediate spin, respectively.

1. Introduction

Metal porphyrins (MPors, Figure 1a) are interesting species because of their great biological importance and the unique nature of their coordination chemistry. (Here we use Por to refer to any porphyrin, regardless of substituents.) As the active centers or prosthetic groups of hemoproteins, iron porphyrins have been extensively studied, both experimentally and theoretically. In the meanwhile, much experimental work has now been done for the analogous manganese complexes. MnPors have been of particular interest in many fields concerning, for example,[1] NMR image enhancement agents, nonlinear optical materials, DNA binding and cleavage agents, radio-diagnostic agents, foodstuff antioxidants, and P-450 cytochrome mimics. In contrast to the case of iron porphyrins, there have been rather few theoretical studies of manganese complexes. A very early calculation on manganese porphine (MnP) was reported by Zerner and Gouterman using the extended Hückel molecular orbital (EHMO) method.[2] Recently, density functional theory (DFT) calculations were carried out for high-valent manganese porphyrins,[3−5] where the oxidation states of Mn are +3 and above. For coordination compounds, the most common oxidation states of Mn are Mn^{II}, Mn^{III}, and Mn^{IV}.[6] The electronic structure of the Mn^{II} porphyrins is not well understood yet. From the early EHMO calculation,[2] a free MnP molecule is predicted to have a quartet ground state. However, a solid sample of manganese tetraphenylporphine (MnTPP)[7] has a magnetic susceptibility indicative of a high-spin configuration (effective magnetic moment $\mu_{eff} = 6.2$ μ_B). Since the EHMO method is rather approximate and limited to only a qualitative analysis based on orbital energies, we think that more accurate calculations on MnP are most desirable.

This paper comprises a detailed DFT study of unligated as well as ligated Mn^{II} porphyrins. For MnPors in solution,

* Corresponding author. E-mail: mhuang@chem.jsums.edu.

(1) (a) Turner, P.; Gunter, M. J.; Skelton, B. W.; White, A. H. *Aust. J. Chem.* **1998**, *51*, 853. (b) Turner, P.; Gunter, M. J. *Inorg. Chem.* **1994**, *33*, 1406.
(2) Zerner, M.; Gouterman, M. *Theor. Chim. Acta* **1966**, *4*, 44.
(3) Ghosh, A.; Gonzalez, E. *Isr. J. Chem.* **2000**, *40*, 1.
(4) Ghosh, A.; Vangberg, T.; Gonzalez, E.; Taylor, P. *J. Porphyrins Phthalocyanines* **2001**, *5*, 345.
(5) de Visser, S. P.; Ogliaro, F.; Gross, Z.; Shaik, S. *Chem.—Eur. J.* **2001**, *7*, 4954.
(6) Boucher, L. J. *Coord. Chem. Rev.* **1972**, *7*, 289.
(7) (a) Gonzalez, B.; Kouba, J.; Yee, S.; Reed, C. A.; Kirner, J. F.; Scheidt, W. R. *J. Am. Chem. Soc.* **1975**, *97*, 3247. (b) Kirner, J. F.; Reed, C. A.; Scheidt, W. R. *J. Am. Chem. Soc.* **1977**, *99*, 1093.

10.1021/ic0401039 CCC: $30.25
Published on Web 02/09/2005

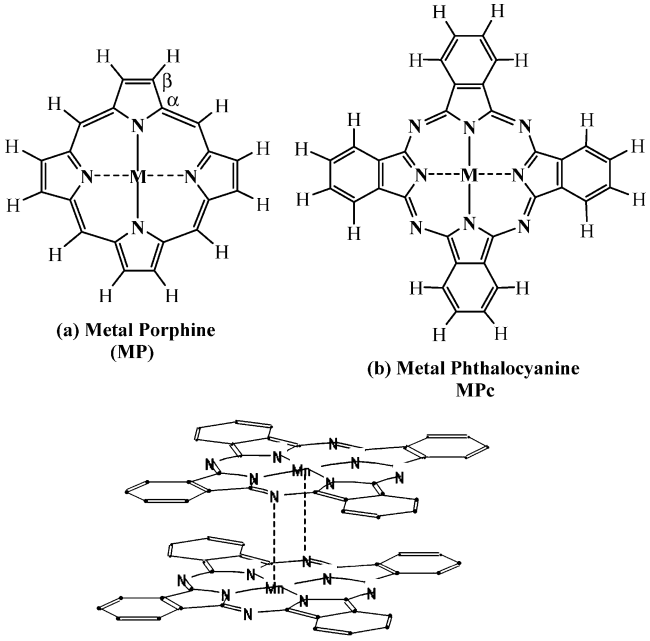

Figure 1. (a) Molecular structure of metal porphine MP. (b) Molecular structure of metal phthalocyanine MPc. (c) Stacking of MnPc molecules in the crystal MnPc structure.

it is very common for the solvent molecules to ligate axially with the metal ion.[6] It is known that axial ligation has a substantial influence on the redox[8,9] and photovoltaic[10] properties of metal porphyrins. The elucidation of the electronic structure and properties of metal porphyrins with axial ligands is also important for understanding their biological and catalytic functions.

To better understand MnPors, our calculations are extended to include manganese phthalocyanines (MnPcs), which are structural analogues of MnPors. Metal phthalocyanines (MPcs, Figure 1b) are in fact another class of fascinating compounds that have found important applications in many fields of science and technology.[11,12] One of the more interesting scientific applications of MPcs is the modeling of biologically important porphyrin-like species. In this regard, MnPc is particularly useful. Although it is generally thought that MPors and MPcs show closely similar behavior, they have many important differences which are exhibited in a striking fashion by the manganese complexes.[6] One major difference between MnPor and MnPc is related to the different spin states of both complexes: the phthalocyanine forms an intermediate-spin, four-coordinate planar complex, while the porphyrin is a high-spin complex that is most likely nonplanar. It would be of interest to make a comparison between MnPors and MnPcs.

On the other hand, some issues and fine details remain to be addressed with MnPcs. From early magnetic susceptibility measurements of MnPc in a crystal,[13] the four-coordinate complex has predominantly a $^4A_{2g}$ ground state arising from the $(b_{2g}/d_{xy})^2(e_g/d_\pi)^2(a_{1g}/d_{z^2})^1$ configuration. But later magnetic circular dichroism (MCD) and ultraviolet−visible (UV−vis) spectroscopy measurements of MnPc in an argon matrix indicated a ^4E_g ground state that corresponds to the $(b_{2g}/d_{xy})^1(e_g/d_\pi)^3(a_{1g}/d_{z^2})^1$ configuration.[14] A $^4A_{2g}$ ground state for MnPc was suggested to be a consequence of intermolecular interactions in the crystal.[14,15] There is also a question as to the electronic structure of the six-coordinate complex of MnPc with pyridine (py), $MnPc(py)_2$. Recently, Janczak et al.[16] reported an X-ray determination of solid $MnPc(py)_2$ and performed a magnetic susceptibility measurement. They argue that their evaluated effective magnetic moment μ_{eff} of $\sim$3.62 μ_B indicates three unpaired electrons ($S = {}^3/_2$), and they assign $MnPc(py)_2$ a $(b_{2g}/d_{xy})^2(e_g/d_\pi)^2(a_{1g}/d_{z^2})^1$ ground-state configuration [a $(a_{1g})^2(e_g)^2(b_{2g})^1$ configuration given originally in their paper[16] is a misprint]. This is different from the results of electron spin resonance (ESR) and magnetic measurements,[17] which "unequivocally" show the complex to be low spin (where $\mu_{eff} = 1.6\ \mu_B$). We note that the axial bond length Mn−N(ax) in solid $MnPc(py)_2$ is only 2.114 Å, much smaller than the Co−N(ax) bond length (2.340 Å) in $CoPc(py)_2$,[16] where an unpaired electron in the $3d_{z^2}$-orbital is responsible for the rather long Co−N(ax) bond. The observed Mn−N(ax) bond length in $MnPc(py)_2$ argues strongly against occupation of the σ-antibonding $3d_{z^2}$-orbital; that is, an intermediate-spin ground state is incompatible with the observed Mn−N(ax) bond length in $MnPc(py)_2$, which requires a low-spin ground state.

The nature of the reduced products of $MnPc(py)_2$ also remains unclear. The experimental observations[17] that there is no significant solvent effect for $[MnPc(py)_2]^-$ and that this ion does not react with CO argue forcefully for the first reduced product to involve reduction of the Pc ring. However, no ESR spectrum observed with this species[17] lends support for a closed-shell ground state for the ion, which implies that the first reduction of $MnPc(py)_2$ involves electron addition to a metal 3d-orbital. The electrochemistry of manganese phthalocyanines has received a good deal of attention[17−21] and may involve both the central metal and the Pc ring. The electronic structures of the oxidized and reduced species were analyzed through their optical spectra,[17−19] but no definite conclusions could be drawn about the ground-state configurations of some of the ions. Another purpose of this paper is to provide a clear description of the

(8) Cocolios, P.; Kadish, K. M. *Isr. J. Chem.* **1985**, *25*, 138.
(9) Takahashi, K.; Komura, T.; Imanaga, H. *Bull. Chem. Soc. Jpn.* **1989**, *62*, 386.
(10) Langford, C. H.; Seto, S.; Hollebone, B. R. *Inorg. Chim. Acta* **1984**, *90*, 221.
(11) *Phthalocyanines: Properties and Applications*; Leznoff, C. C., Lever, A. B. P., Eds.; VCH Publishers: New York, 1996; Vol. 4.
(12) Chambrier, I.; Cook, M. J.; Wood, P. T. *Chem. Commun.* **2000**, 2133.
(13) (a) Barraclough, C. G.; Martin, R. L.; Mitra, S.; Sherwood, R. C. *J. Chem. Phys.* **1970**, *53*, 1638. (b) Mitra, S.; Gregson, A. K.; Hatfield, W. E.; Weller, R. R. *Inorg. Chem.* **1983**, *22*, 1729.
(14) Williamson, B. E.; VanCott, T. C.; Boyle, M. E.; Misener, G. C.; Stillman, M. J.; Schatz, P. N. *J. Am. Chem. Soc.* **1992**, *114*, 2412.
(15) Reynolds, P. A.; Figgis, B. N. *Inorg. Chem.* **1991**, *30*, 2294.
(16) Janczak, J.; Kubiak, R.; Śledź, M.; Borrmann, H.; Grin, Y. *Polyhedron* **2003**, *22*, 2689.
(17) Lever, A. B. P.; Minor, P. C.; Wilshire, J. P. *Inorg. Chem.* **1981**, *20*, 2550.
(18) Minor, P. C.; Gouterman, M.; Lever, A. B. P. *Inorg. Chem.* **1985**, *24*, 1894.
(19) Clack, D. W.; Yandle, J. R. *Inorg. Chem.* **1972**, *11*, 1738.
(20) Komorsky-Lovrić, Š. *J. Electroanal. Chem.* **1995**, *397*, 211.
(21) Lin, C.-L.; Lee, C.-C.; Ho, K.-C. *J. Electroanal. Chem.* **2002**, *524*, 81.

ground states for the $[MnPor/Pc]^{x\pm}$ and $[MnPor/Pc(py)_2]^{x\pm}$ ions ($x = 1, 2$).

2. Computational Details

The molecular structure of the simplest metal porphyrin, metal porphine (MP), is illustrated in Figure 1a. The systems that have been synthesized contain phenyl or ethyl groups as substituents on the periphery of the porphyrin ring. The use of MP as a model for larger and more complicated systems has been justified in previous calculations,[22] which show that the electronic properties of metal porphyrins are insensitive to the nature of these peripheral substituents.

Figure 1b shows the molecular structure of the metal phthalocyanine (MPc). In the lower part of Figure 1 (i.e. Figure 1c), we also exhibit the arrangement of discrete, planar MnPc molecules in the β-phase crystal structure of MnPc,[23] where two *aza* nitrogen atoms of each molecule lie exactly above or below the metal belonging to their nearest neighbors. The distance between these axially located nitrogen atoms and the Mn atom is about 3.2 Å. It was argued that the intermolecular interaction, particularly the weak axial ligation, may cause the crystal ground state to differ from that of the free molecule.[14,15] To examine the effect of the *aza* nitrogens of adjacent molecules on the electronic state of MnPc, we calculated a model system MnPc$\cdots(HCN)_2$, where the two HCN molecules were placed separately above and below the central Mn with Mn$\cdots$N$-$C$-$H in a linear arrangement, perpendicular to the macrocycle plane; the Mn$\cdots$N distance was fixed at 3.2 Å.

All calculations were based on the Amsterdam density functional (ADF) program package (version 2.0.1) developed by Baerends and co-workers.[24] The Slater-type orbital (STO) basis used for the valence shells is of triple-ζ quality plus one polarization function for all atoms; single-ζ STOs are used for core orthogonalization. The frozen core assigned for Mn consisted of 1s2s2p; the valence set on the metal includes $(n - 1)$ s and $(n - 1)$ p shells. For C and N, the [He] core definition was used. Among the various exchange-correlation potentials available, the density-parametrization form of Vosko, Wilk, and Nusair (VWN),[25] Becke's gradient correction for exchange (B),[26] and Perdew's gradient correction for correlation (P)[27] were employed. It has been shown that the combined VWN$-$B$-$P functional approach can provide accurate bonding energies for both main group[28] and transition metal[29] systems. Relativistic corrections of the valence electrons were calculated by the quasi-relativistic (QR) method attributed to Ziegler et al.[30] For the open-shell states, the unrestricted Kohn$-$Sham (UKS) spin-density functional approach was adopted.

Since the present implementation of DFT which utilizes Kohn$-$Sham orbitals is based on a single determinant, one has to be aware of the limitations of the DFT method, as noted in refs 4 and 5. DFT often yields incorrect ordering of spin states for transition metals, especially in situations of s^1d^{n-1} versus d^n configurations.[5] These deficiencies would disappear in transition metal complexes in which the metal s-orbital is no longer available.[5] This is the situation for the systems studied here. Although the DFT method is not generally applicable to excited states, it can be used to good effect to calculate the lowest energy state of each symmetry for a particular system.[31] There have been many applications of DFT methods to the calculations of excited states in unligated and ligated iron porphyrins (e.g. refs 32a$-$e). To assess the validity of the ADF method used in this work, calculations on iron porphine (FeP) have also been carried out, and a comparison of the results from different computational methods is reported in the Supporting Information. The success of ADF calculations on iron porphyrins lends confidence in applying the same program to the manganese porphyrins.

3. Results and Discussion

Experiment and calculation have established that simple transition metal porphines (MPs) have a planar D_{4h} symmetry.[33] The crystal structure of MPc indicates that the molecule is not perfectly square planar,[23] but its symmetry is almost surely D_{4h} in solution[34] and in the gas phase.[35] Assuming MnP and MnPc are planar, D_{4h} symmetry was imposed in the calculations on both molecules. We chose a coordinate system with the x and y axes passing through the pyrrole N atoms and the Mn atom, with the z axis perpendicular to the plane of the molecule. In the D_{4h} point group, the metal 3d-orbitals are classified as b_{2g} (d_{xy}), e_g (d_π, i.e., d_{xz} and d_{yz}), a_{1g} (d_{z^2}), and b_{1g} ($d_{x^2-y^2}$). For a d^5 ion in a D_{4h} ligand field, there are a number of possible low-lying states. The purpose of this paper is to elucidate the ground state and several low-lying excited states that are usually considered in the literature. Geometry optimization was performed for all states of each molecule. The calculated relative energies of the various states for MnP and MnPc are collected in Table 1, together with the optimized equatorial Mn$-$N bond lengths ($R_{Mn-N(eq)}$) of each state. Table 2 displays the calculated Mn$-$P/Pc binding energies (E_{bind}), ionization potentials (IP), electron affinities (EA), and Mulliken charge distributions on Mn (Q_{Mn}). E_{bind} is defined as the energy required to separate the metal (neutral) from the ring (neutral):

$$-E_{bind} = E(MnP/Pc) - \{E(Mn) + E(P/Pc)\}$$

The IPs and EAs were calculated by the so-called ΔSCF method which carries out separate SCF (self-consistent field)

(22) Liao, M.-S.; Scheiner, S. *J. Chem. Phys.* **2002**, *117*, 205.
(23) (a) Kirner, J. F.; Dow, W.; Scheidt, W. R. *Inorg. Chem.* **1976**, *15*, 1685. (b) Mason, R.; Williams, G. A.; Fielding, P. E. *J. Chem. Soc., Dalton Trans.* **1979**, 676.
(24) (a) Baerends, E. J.; Ellis, D. E.; Ros, P. *Chem. Phys.* **1973**, *2*, 41. (b) te Velde, G.; Baerends, E. J. *J. Comput. Phys.* **1992**, *99*, 84.
(25) Vosko, S. H.; Wilk, L.; Nusair, M. *Can. J. Phys.* **1980**, *58*, 1200.
(26) Becke, A. D. *Phys. Rev. A* **1988**, *38*, 3098.
(27) Perdew, J. P. *Phys. Rev. B* **1986**, *33*, 8822.
(28) Johnson, B. G.; Gill, P. M. W.; Pople, J. A. *J. Chem. Phys.* **1993**, *98*, 5612.
(29) Li, J.; Schreckenbach, G.; Ziegler, T. *J. Am. Chem. Soc.* **1995**, *117*, 486.
(30) Ziegler, T.; Tschinke, V.; Baerends, E. J.; Snijders, J. G.; Ravenek, W. *J. Phys. Chem.* **1989**, *93*, 3050.
(31) (a) Jones, R. O.; Gunnarson, O. *Rev. Mod. Phys.* **1989**, *61*, 689. (b) Ziegler, T.; Rauk, A.; Baerends, E. J. *Theor. Chim. Acta* **1977**, *43*, 261.
(32) (a) Delley, B. *Physica B* **1991**, *172*, 185. (b) Matsuzawa, N.; Ata, M.; Dixon, D. A. *J. Phys. Chem.* **1995**, *99*, 7698. (c) Rovira, C.; Kunc, K.; Hutter, J.; Ballone, P.; Parrinello, M. *J. Phys. Chem. A* **1997**, *101*, 8914. (d) Kozlowski, P. M.; Spiro, T. G.; Bérces, A.; Zgierski, Z. *J. Phys. Chem. B* **1998**, *102*, 2603. (e) Kozlowski, P. M.; Spiro, T. G.; Zgierski, M. Z. *J. Phys. Chem. B* **2000**, *104*, 10659.
(33) (a) Rosa, A.; Ricciardi, G.; Baerends, E. J.; van Gisbergen, S. J. A. *J. Phys. Chem. A* **2001**, *105*, 3311. (b) Nguyen, K. A.; Pachter, R. *J. Chem. Phys.* **2001**, *114*, 10757.
(34) Kahl, J. L.; Faulkner, L. R.; Dwarakanath, K.; Tachikawa, H. *J. Am. Chem. Soc.* **1986**, *108*, 5434.
(35) Ruan, C.-Y.; Mastryukov, V.; Fink, M. *J. Chem. Phys.* **1999**, *111*, 3035.

Table 1. Calculated Relative Energies (E, eV) and Mn−N(eq) Bond Lengths (R, Å) for Different Configurations in MnP and MnPc (eq = equatorial)

configuration[a]					MnP		MnPc	
b_{2g}/d_{xy}	$1e_g$/d_π	a_{1g}/d_{z^2}	b_{1g}/$d_{x^2-y^2}$	state	E	$R_{Mn-N(eq)}$	E[b]	$R_{Mn-N(eq)}$
1	3	1	0	^4E_g	0	1.995	0 (0)	1.931
2	2	1	0	$^4A_{2g}$	0.16	1.992	0.32 (0.14)	1.935
1	2	1	1	$^6A_{1g}$	0.45	2.059	1.09 (1.33)	1.998
1	4	0	0	$^2B_{2g}$	1.69	2.003	1.64 (1.65)	1.942
2	3	0	0	^2E_g	2.08	1.997	2.11 (2.24)	1.941

[a] Orbital energy levels illustrated in Figure 3. [b] The values in parentheses are those calculated for MnPc···$(HCN)_2$ ($R_{Mn\cdots N(ax)}$ = 3.2 Å; see text). The optimized Mn−N(eq) bond lengths for the model system are nearly the same as those for MnPc.

Table 2. Calculated Mn−P/Pc Bind Energies (E_{bind}), Ionization Potentials (IP), Electron Affinities (EA), and Mulliken Charge Distributions on Mn (Q_{Mn})

	MnP (^4E_g)	MnP ($^6A_{1g}$)	MnPc (^4E_g)
E_{bind}, eV	9.22	8.77	8.80
IP, eV	5.65 ($1e_g/d_\pi$)	5.38 ($b_{1g}/d_{x^2-y^2}$)	5.93 ($1e_g/d_\pi$)
	7.03 (a_{2u})	6.90 (a_{2u})	6.51 (a_{1u})
	7.03 (a_{1u})	7.01 (a_{1u})	
EA, eV	−1.86 ($1e_g/d_\pi$)	−1.58 ($1e_g/d_\pi$)	−2.79 ($1e_g/d_\pi$)
	−1.41 (b_{2g}/d_{xy})	−0.32 (a_{1g}/d_{z^2})	−2.14 (b_{2g}/d_{xy})
	−1.28 (a_{1g}/d_{z^2})		−2.04 (a_{1g}/d_{z^2})
Q_{Mn}, e	0.89	0.88	0.96

calculations for the neutral molecule and its ion, where EA = $E(X^-) - E(X)$.

3.1. MnP. Before discussing the electronic states of MnP, we first give a brief description of the experimental results on the unligated manganese^{II} porphyrin. As early as the 1970s, Reed et al. reported X-ray determinations on crystalline manganese tetraphenylporphine (MnTPP).[7] The (average) Mn−N bond length is given in the range of 2.082−2.092 Å, depending on the assumptions made in interpreting the least-squares refinements. A refinement of the diffraction data with the Mn^{II} atom positioned at the inversion center leads to an unrealistically large thermal parameter (root-mean-square displacement 0.35 Å). A second refinement in which the Mn^{II} atom was allowed to take an out-of-plane position gives rise to a less unrealistic thermal parameter. Either alternative suggests that MnTPP is nonplanar with the metal atom out of the porphyrin plane. Magnetic susceptibility measurements of the solid sample yield an effective magnetic moment of 6.2−6.6 μ_B, indicating five unpaired 3d-electrons for Mn^{II}. The measured Mn−N(eq) bond length is also readily interpreted in terms of a high-spin ($S = {}^5/_2$) ground state. It was argued that the out-of-plane displacement may be either a static or dynamic process.

Let us examine the calculated results. For planar MnP, the intermediate-spin quartet ^4E_g [$(d_{xy})^1(d_\pi)^3(d_{z^2})^1$] was computed to be the lowest in energy. This is *not* different from the early EHMO result,[2] which predicts that the Mn^{II} ion must be intermediate spin in order to be in the plane. The high-spin sextet $^6A_{1g}$ lies 0.45 eV higher. This result would appear to disagree with the assignment of a high-spin ground state for this type of molecule. As mentioned above, the Mn^{II} atom in MnTPP was predicted to lie out of the porphyrin plane. We thus examined the change of the (relative) energy (E) of MnP with the motion of the metal out of the plane

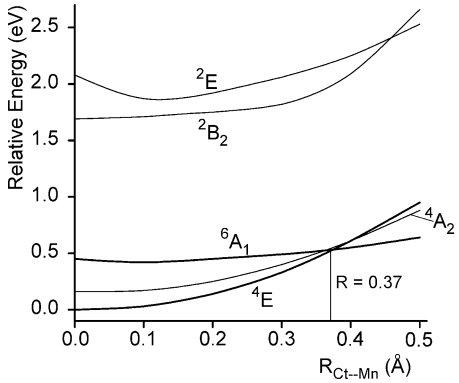

Figure 2. Variation of the relative state energy with the Mn out-of-plane displacement in MnP.

($R_{Ct\cdots Mn}$, which denotes the distance between the center of the ring, Ct, and the Mn). For each spin state and each fixed R, the structure of MnP was reoptimized in C_{4v} symmetry. The potential curves of the various spin states are illustrated in Figure 2. The detailed calculated data show that the potential curve of the high-spin $^6A_1$ state has a local minimum at $R_{Ct\cdots Mn}$ = 0.1 Å, but the decrease of the energy from $R_{Ct\cdots Mn}$ = 0 Å to $R_{Ct\cdots Mn}$ = 0.1 Å is so small (0.01 eV) that it may be negligible. The energies of the ^4E and $^4A_2$ states are lower than that of the $^6A_1$ state near the equilibrium and go up monotonically with $R_{Ct\cdots Mn}$. These results imply that the Mn^{II} atom in the free MnP molecule has no obvious tendency to move out of the porphyrin plane for both intermediate- and high-spin states. The lowest quartet (^4E) curve intersects with $^6A_1$ at $R_{Ct\cdots Mn} \sim 0.37$ Å, indicating a switch to high spin at this degree of nonplanarity. The Mn^{II} out-of-plane displacement in the crystal MnTPP is estimated to be ~0.19 Å,[7] somewhat smaller than the calculated one. The comparison between the calculated and experimental $R_{Ct\cdots Mn}$ values would suggest that the ADF method probably overestimates the high-spin state energy by about 0.3−0.4 eV. It is possible that the crystal packing forces in solid MnTPP perturb the Mn^{II} atom away from the porphyrin center and make the molecule high spin.

Figure 3 illustrates the valence molecular orbital (MO) energy levels of MnP in both the ^4E_g and $^6A_{1g}$ states, obtained by spin-restricted calculations. It is shown that four occupied 3d-like orbitals b_{2g} (d_{xy}), $1e_g$ (d_π), and a_{1g} (d_{z^2}) fall well above the a_{2u}-orbital, the highest occupied MO (HOMO) of the porphyrin ring. The antibonding $d_{x^2-y^2}$-orbital (b_{1g}) is particularly destabilized through its interaction with the porphyrin nitrogens. The empty porphyrin $2e_g$ (π^*) is the lowest unoccupied MO (LUMO); it contains a contribution of 12% from the metal d_π. A rather strong porphyrin−metal π mixing was suggested to be responsible for the anomalous, intense nature of the charge-transfer bands for M^{III} porphyrins,[6] and the calculation provides support for this suggestion. In the ^4E_g state, the d_π and d_{z^2}-orbitals, which are nearly degenerate, are weakly antibonding, are higher in energy than the nonbonding d_{xy}-orbital, and represent a group of HOMOs. In the high-spin $^6A_{1g}$ state, however, the d_{xy}-orbital is greatly destabilized, owing to the repulsion interaction with the electron of $d_{x^2-y^2}$, which pushes the d_{xy}-orbital even higher than both d_{z^2} and d_π. The a_{2u}- and a_{1u}-orbitals, which are

Table 3. Calculated Relative Energies (E, eV) for Selected Configurations in $[MnP/Pc]^{x\pm}$ and $[MnP/Pc(py)_2]^{x\pm}$ ($x = 1, 2$)

	configuration[a]	term	E	redox products[b]
$[MnP]^{1+}$	$(a_{2u})^2(b_{2g})^1(1e_g)^2(a_{1g})^1$	$^5B_{1g}$	0	$[Mn^{III}P]^{1+}$
	$(a_{2u})^1(b_{2g})^1(1e_g)^3(a_{1g})^1$	^5E_u	1.38	
$[MnP]^{2+}$	$(a_{2u})^1(b_{2g})^1(1e_g)^2(a_{1g})^1$	$^6B_{2u}$	0	$[Mn^{III}P]^{2+}$
	$(a_{2u})^2(b_{2g})^1(1e_g)^1(a_{1g})^1$	^4E_g	0.86	
	$(a_{2u})^2(b_{2g})^1(1e_g)^2(a_{1g})^0$	$^4B_{1g}$	2.62	
$[MnP]^{1-}$	$(b_{2g})^1(1e_g)^4(a_{1g})^1$	$^3B_{2g}$	0	$[Mn^{I}P]^{1-}$
	$(b_{2g})^1(1e_g)^3(a_{1g})^1(2e_g)^1$	$^5B_{1g}$	0.57	
$[MnP]^{2-}$	$(b_{2g})^1(1e_g)^4(a_{1g})^1(2e_g)^1$	^4E_g	0	$[Mn^{I}P]^{2-}$
	$(b_{2g})^2(1e_g)^4(a_{1g})^1$	$^2A_{1g}$	0.03	
	$(b_{2g})^1(1e_g)^3(a_{1g})^1(2e_g)^2$	^6E_g	0.43	
$[MnPc]^{1+}$	$(b_{2g})^1(a_{1u})^2(1e_g)^2(a_{1g})^1$	$^5B_{1g}$	0	$[Mn^{III}Pc]^{1+}$
	$(b_{2g})^1(a_{1u})^1(1e_g)^3(a_{1g})^1$	^5E_u	0.58	
$[MnPc]^{2+}$	$(b_{2g})^1(a_{1u})^1(1e_g)^2(a_{1g})^1$	$^6B_{1u}$	0	$[Mn^{III}Pc]^{2+}$
	$(b_{2g})^1(a_{1u})^2(1e_g)^1(a_{1g})^1$	^4E_g	1.19	
$[MnPc]^{1-}$	$(b_{2g})^1(a_{1u})^2(1e_g)^4(a_{1g})^1$	$^3B_{2g}$	0	$[Mn^{I}Pc]^{1-}$
	$(b_{2g})^1(a_{1u})^2(1e_g)^3(a_{1g})^1(2e_g)^1$	$^5B_{1g}$	0.68	
$[MnPc]^{2-}$	$(b_{2g})^1(a_{1u})^2(1e_g)^4(a_{1g})^1(2e_g)^1$	^4E_g	0	$[Mn^{I}Pc]^{2-}$
	$(b_{2g})^2(a_{1u})^2(1e_g)^4(a_{1g})^1$	$^2A_{1g}$	0.17	
	$(b_{2g})^1(a_{1u})^2(1e_g)^3(a_{1g})^1(2e_g)^2$	^6E_g	0.56	
$[MnP(py)_2]^{1+}$	$(b_{1u})^2(1a_{1g})^1(1b_{3g})^2(1b_{2g})^1$	$^3B_{2g}$	0	$[Mn^{III}P(py)_2]^{1+}$
	$(b_{1u})^1(1a_{1g})^1(1b_{3g})^2(1b_{2g})^2$	$^3B_{1u}$	1.19	
$[MnP(py)_2]^{2+}$	$(b_{1u})^2(1a_{1g})^1(1b_{3g})^1(1b_{2g})^1$	$^4B_{1g}$	0	$[Mn^{IV}P(py)_2]^{2+}$
	$(b_{1u})^1(1a_{1g})^1(1b_{3g})^2(1b_{2g})^1$	$^4B_{3u}$	0.60	
$[MnP(py)_2]^{1-}$	$(1a_{1g})^2(1b_{3g})^2(1b_{2g})^2$	$^1A_{1g}$	0	$[Mn^{I}P(py)_2]^{1-}$
	$(1a_{1g})^1(1b_{3g})^2(1b_{2g})^2(2b_{2g})^1$	$^3B_{2g}$	0.34	
$[MnP(py)_2]^{2-}$	$(1a_{1g})^2(1b_{3g})^2(1b_{2g})^2(2b_{2g})^1$	$^2B_{2g}$	0	$[Mn^{I}P(py)_2]^{2-}$
	$(1a_{1g})^1(1b_{3g})^2(1b_{2g})^2(2b_{2g})^1(2b_{3g})^1$	$^4B_{1g}$	0.26	
$[MnPc(py)_2]^{1+}$	$(a_{1u})^2(1a_{1g})^1(1b_{3g})^2(1b_{2g})^1$	$^3B_{2g}$	0	$[Mn^{III}Pc(py)_2]^{1+}$
	$(a_{1u})^1(1a_{1g})^1(1b_{3g})^2(1b_{2g})^2$	$^3A_{1u}$	0.48	
$[MnPc(py)_2]^{2+}$	$(a_{1u})^1(1a_{1g})^1(1b_{3g})^2(1b_{2g})^1$	$^4B_{2u}$	0	$[Mn^{III}Pc(py)_2]^{2+}$
	$(a_{1u})^2(1a_{1g})^1(1b_{3g})^1(1b_{2g})^1$	$^4B_{1g}$	0.02	
$[MnPc(py)_2]^{1-}$	$(1a_{1g})^2(1b_{3g})^2(1b_{2g})^2$	$^1A_{1g}$	0	$[Mn^{I}Pc(py)_2]^{1-}$
	$(1a_{1g})^1(1b_{3g})^2(1b_{2g})^2(2b_{2g})^1$	$^3B_{2g}$	0.35	
$[MnPc(py)_2]^{2-}$	$(1a_{1g})^2(1b_{3g})^2(1b_{2g})^2(2b_{2g})^1$	$^2B_{2g}$	0	$[Mn^{I}Pc(py)_2]^{2-}$
	$(1a_{1g})^1(1b_{3g})^2(1b_{2g})^2(2b_{2g})^1(2b_{3g})^1$	$^4B_{1g}$	0.20	

[a] Orbital energy levels illustrated in Figure 3. [b] Oxidation or reduction products.

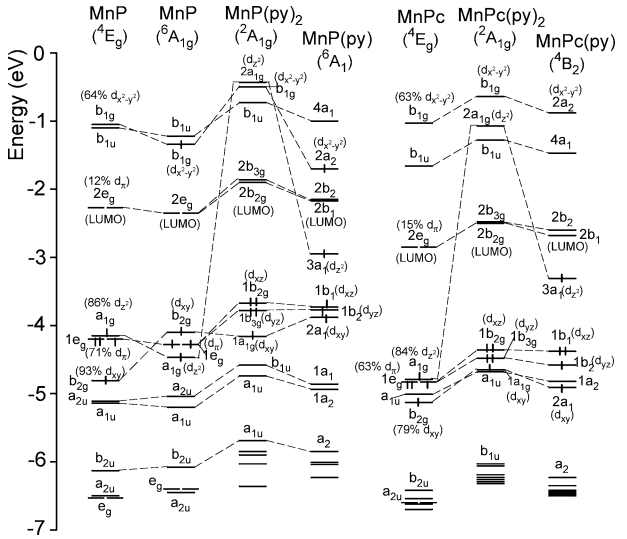

Figure 3. Valence molecular orbital energy levels of MnP/Pc, MnP/Pc(py)$_2$, and MnP/Pc(py) (Mulliken populations of the Mn 3d-orbitals are indicated in parentheses).

nearly degenerate in the ^4E_g state, are separated significantly in the $^6A_{1g}$ state. The calculated Mn−N(eq) bond length for the high-spin state (2.06 Å) is quite comparable to that measured in the crystal MnTPP (2.08−2.09 Å), where the occupancy of $d_{x^2-y^2}$ causes an expansion of the porphyrin core by about 0.06 Å according to the calculation.

In Table 2, calculated properties of MnP are also presented for both the ^4E_g and $^6A_{1g}$ states (it is unclear whether the molecule is intermediate spin or high spin when it is in the gas phase or solution). The Mn−P binding energy is estimated to be ∼9.2 eV, which is ∼1 eV weaker than that of FeP (see the Supporting Information). The first IP is slightly different for different spin states, that is, 5.65 eV for ^4E_g and 5.38 eV for $^6A_{1g}$. The same situation happens for the calculated EA. The first ionization occurs apparently from a metal d-orbital, while the IP from the porphyrin a_{2u}-orbital is more than 1 eV higher. $[MnP]^+$ has a $^5B_{1g}$ [$(d_{xy})^1(d_\pi)^2(d_{z^2})^1$] ground state, whether the neutral molecule is intermediate spin or high spin. Further ionization (or oxidation) to $[MnP]^{2+}$ now extracts an electron from the ring a_{2u}. Concerning reduction, the first electron is added to the low-lying, partially filled ($1e_g/d_\pi$) level. The second reduction may involve addition of an electron to either P $2e_g$ (π^*) or Mn b_{2g} (d_{xy}), because the respectively resulted ^4E_g and $^2A_{1g}$ states are nearly degenerate. The calculated relative energies for selected configurations in $[MnP]^{x\pm}$ ($x = 1, 2$) are reported in Table 3.

3.2. MnPc. Owing to the smaller core size of the Pc ring, the energy separation between the ^4E_g and $^6A_{1g}$ states for MnPc (1.09 eV) is significantly larger than that for MnP. The calculation indicates that the ground state of MnPc is ^4E_g, arising from the $(d_{xy})^1(d_\pi)^3(d_{z^2})^1$ configuration, in agreement with the more recent MCD and UV−vis measurements of MnPc in an argon matrix;[14] the $^4A_{2g}$ state is 0.32 eV higher in energy than the ^4E_g state. The calculated Mn−N(eq) bond

length for the ground state (1.931 Å) is also nearly equal to that obtained from the crystal structure (1.933 Å).[23] Thus MnPc is classified as an intermediate-spin system, as its measured effective magnetic moment shows (μ_{eff} = 4.33 μ_B).[13]

As previously mentioned, the results of magnetic measurements on the β-phase solid MnPc indicate a $^4A_{2g}$ [$(d_{xy})^2(d_\pi)^2(d_{z^2})^1$] ground state, which was attributed to the fact that there are *aza* nitrogen atoms of adjacent parallel molecules lying above and below the Mn^{II} atom in the crystal. To examine the effect of the two axially located nitrogens, we calculated a model system MnPc···$(HCN)_2$ with the axial Mn···N(ax) distance equal to that in the crystal (3.2 Å). The calculated relative energies for the different configurations are displayed in parentheses in Table 1. In such a coordination, the relative energy of the $^4A_{2g}$ state is decreased by 0.18 eV, which seems not to be enough to make this state become the ground state. This may imply that in addition to the *aza* nitrogens, the other atoms within the adjacent molecules may also have a significant influence on the electronic structure of MnPc. We note that in contrast to the energy decrease for $^4A_{2g}$, the other state energies are more or less increased upon adding the HCN molecules in the axial positions.

The MO energy level diagram of MnPc is presented in the right-hand part of Figure 3. Compared to the case of P, the *aza* nitrogen atoms in Pc lower the energies of the valence MOs, particularly a_{2u} (as this orbital is mainly concentrated in the *meso* position).[36] The smaller core size of Pc splits the metal $d_{x^2-y^2}$ away from the other d-orbitals to a greater extent than does P. Since the a_{1u}-orbital contains a large contribution from the β-carbon, the tetrabenzo annulations cause a large energy shift for the a_{1u}-orbital so that this orbital lies above the d_{xy}-orbital in MnPc.

The Mn−Pc binding energy of 8.8 eV is somewhat smaller than that of Mn−P. This trend is different from the early EHMO prediction based on the Mulliken charge distributions which suggest that MPc is more stable than MP. Here we show that the smaller core size of Pc does not give rise to a larger ligand field. This is because the benzo annulation produces a surprisingly strong destabilizing effect on the metal−macrocycle bonding.[37]

Corresponding to the downshift/upshift of the valence MOs, the calculated IPs are higher/lower than those of MnP; for example, the IP from the d_π-orbital is increased by ∼0.3 eV from MnP to MnPc, while the IP from the a_{1u}-orbital is decreased by ∼0.5 eV. Nevertheless, the first ionization in MnPc also occurs at the central metal (d-orbital), similar to the case of MnP but different from the situation of FeP versus FePc (see the Supporting Information). The EA of MnPc is significantly larger than that of MnP; the same is true for the ligated complexes (see section 3.3.1). This is reflected in the electrochemical data:[17] reduction of the manganese phthalocyanine complex appears 0.5−0.8 V anodic of the corresponding porphyrin.

The oxidation and reduction patterns of MnPc are similar to those of MnP; namely, the redox products are $[Mn^{III}Pc]^{x+}$ and $[Mn^{I}Pc]^{x-}$ (x = 1, 2). Clack and Yandle suggested,[19] based on the experimental observation that the absorption spectra for all stages of reduction for MnPc are very similar to the corresponding spectra of both MgPc and ZnPc, that the reduction pattern for MnPc follows the same sequence as that of MgPc or ZnPc with all electrons assigned to the Pc $2e_g$-orbitals. According to the calculations, however, MnPc reduces initially to form $[Mn^{I}Pc]^-$ where the additional electron enters a Mn d-orbital (d_π); the subsequent reduction occurs into the Pc $2e_g$-orbital. That is, the Mn in $[MnPc]^-$ and $[MnPc]^{2-}$ does not revert to a 2+ oxidation state, which therefore does not support the above suggestion of Clack and Yandle. Recent electrochemical experimental results[20,21] which indicate the oxidation states Mn^{III} for $[MnPc]^+$ and Mn^{I} for $[MnPc]^-$ are consistent with the calculations.

3.3. Axial Ligation of Pyridine (py). Extra coordination, that is, attachment of the fifth and sixth ligands along the *z*-axis, is an important property of four-coordinate metal porphyrins/phthalocyanines. The electronic structures and properties of these complexes are sensitive to the nature and number of the axial ligands.[8,9] Conversely, the nature of the tetrapyrrole macrocycle can also influence the chemistry at the metal and its interaction with an axial ligand (L). For example, MnPc has been reported to add two ligands to form low-spin, six-coordinate $MnPc(L)_2$ species;[6,17,18] MnPor, on the other hand, has the preference of adding only one ligand to form high-spin, five-coordinate MnPor(L) species.[7] To better understand the chemistry of the ligated derivatives of MnPor and MnPc, the properties of $MnP/Pc(py)_2$ and MnP/Pc(py) were examined here, where py represents a popular axial ligand that binds well with transition metals. The orientation of the py ligand was such that the py ring plane is perpendicular to the macrocycle and bisects the N−Mn−N angles of the latter. The symmetries of the six- and five-coordinate complexes are D_{2h} and C_{2v}, respectively. Effects of the axial ligands upon the various MO levels of MnP/Pc are illustrated in Figure 3.

3.3.1. $MnP(py)_2$ and $MnPc(py)_2$. The calculated relative energies and structural parameters for different configurations in $MnP/Pc(py)_2$ are collected in Table 4, where $R_{Mn-N(eq)}$ and $R_{Mn-N(ax)}$ denote the equatorial and axial Mn−N bond lengths, respectively. The states are listed in the same order as in the earlier tables, to more clearly emphasize changes in the energy ordering caused by the axial ligation. Geometry optimization reveals that there are rather long Mn−N(ax) bond lengths for the states with a singly occupied d_{z^2}-orbital, with the $R_{Mn-N(ax)}$ values being 2.45−2.46 Å in $MnP(py)_2$ and 2.48 Å in $MnPc(py)_2$. According to Table 4, both complexes adopt a low-spin $^2A_{1g}$ ($^2B_{2g}$) ground state (parentheses indicate the corresponding states in MnP/Pc). There are X-ray crystal structure data available for $MnPc(py)_2$,[16] wherein $R_{Mn-N(eq)}$ = 1.954 Å and $R_{Mn-N(ax)}$ = 2.114 Å. These values compare favorably with the calculated ones in the ground state (1.948 and 2.072 Å, respectively). Thus the recent assignment of an intermediate-spin ground state for this complex[16] proves to be incorrect, since the suggested $(d_{xy})^2(d_\pi)^2(d_{z^2})^1$ configuration would result in a much longer Mn−N(ax) bond length. On the other hand, the earlier

(36) Liao, M.-S.; Scheiner, S. *Chem. Phys. Lett.* **2003**, *367*, 199.
(37) Liao, M.-S.; Scheiner, S. *J. Comput. Chem.* **2002**, *23*, 1391.

Table 4. Calculated Relative Energies (E) and Structural Parameters (R) for Different Configurations in $MnP(py)_2$ and $MnPc(py)_2$

configuration								
$1a_{1g}/d_{xy}$	$1b_{3g}/d_{yz}$	$1b_{2g}/d_{xz}$	$2a_{1g}/d_{z^2}$	$b_{1g}/d_{x^2-y^2}$	state[a]	E (eV)	$R_{Mn-N(eq)}$[b] (Å)	$R_{Mn-N(ax)}$[b] (Å)
(a) $MnP(py)_2$								
1	1	2	1	0	$^4B_{3g}$ (^4E_g)	0.47	2.005	2.450
2	1	1	1	0	$^4B_{1g}$ ($^4A_{2g}$)	0.92	2.006	2.463
1	1	1	1	1	$^6A_{1g}$ ($^6A_{1g}$)	0.88	2.085	2.460
1	2	2	0	0	$^2A_{1g}$ ($^2B_{2g}$)	0	2.005	2.061
2	1	2	0	0	$^2B_{3g}$ (^2E_g)	0.20	2.002	2.060
(b) $MnPc(py)_2$								
1	1	2	1	0	$^4B_{3g}$ (^4E_g)	0.59	1.945	2.483
2	1	1	1	0	$^4B_{1g}$ ($^4A_{2g}$)	1.17	1.950	2.478
1	1	1	1	1	$^6A_{1g}$ ($^6A_{1g}$)	1.58	2.026	2.482
1	2	2	0	0	$^2A_{1g}$ ($^2B_{2g}$)	0	1.948	2.072
2	1	2	0	0	$^2B_{3g}$ (^2E_g)	0.32	1.950	2.070
exptl distances in crystal $MnPc(py)_2$ (ref 16):							1.954	2.114

[a] States in parentheses are the corresponding states in unligated MnP/Pc. [b] Equatorial is denoted eq; axial is denoted ax.

Table 5. Calculated Properties of MnP/Pc and $MnP/Pc(py)_2$ in the Ground State

	MnP (^4E_g)	$MnP(py)_2$ ($^2A_{1g}$)	MnPc (^4E_g)	$MnPc(py)_2$ ($^2A_{1g}$)
$R_{Mn-N(eq)}$, Å	1.995	2.005	1.931	1.948
$R_{Mn-N(ax)}$, Å		2.061		2.072
Q_{Mn}, e	0.89	0.91	0.96	0.94
$Q_{(py)}$, e		0.18		0.22
E_{bind}[MnP/Pc$-$(py)$_2$],[a] eV		1.11		1.33
E_{diss}[$-$(py)$_2$ $\rightarrow$ $-$(py) + py],[b] eV		0.59		0.82
IP, eV	5.65 ($1e_g/d_\pi$)	5.21 ($1b_{2g}/d_{xz}$)	5.93 ($1e_g/d_\pi$)	5.63 ($1b_{2g}/d_{xz}$)
		5.29 ($1b_{3g}/d_{yz}$)		5.72 ($1b_{3g}/d_{yz}$)
		6.40 (b_{1u})		6.11 (a_{1u})
EA, eV	$-$1.86 ($1e_g/d_\pi$)	$-$1.36 ($1a_{1g}/d_{xy}$)	$-$2.79 ($1e_g/d_\pi$)	$-$2.11 ($1a_{1g}/d_{xy}$)
		$-$1.02 ($2b_{2g}$)		$-$1.76 ($2b_{2g}$)

[a] Binding energy between MnP/Pc and two py ligands. [b] Dissociation energy $-E_{diss}$ = MnP/Pc(py)$_2$ $-$ [MnP/Pc(py) + py].

ESR and UV$-$vis spectra of $MnPc(py)_2$ in solution indicated a low-spin complex with a metal d-orbital population $(d_{xy})^1(d_\pi)$,[4,6,17] which is then supported by the calculation. The magnetic measurements of the solid $MnPc(py)_2$ by Janczak et al.[16] yielded an effective magnetic moment of $\sim$3.62 μ_B, which was thought by these authors to support their intermediate-spin state. However, the significantly larger value of the measured μ_{eff} versus the spin-only value for $S = {}^1/_2$ (1.73 μ_B) may be due to the fact that the starting $MnPc(py)_2$ solid sample was not entirely pure (as pointed out by Janczak et al.[16]) and oxidized compounds were present.

Compared to those in MnP/Pc, the orbitals in $MnP/Pc(py)_2$ are shifted upward, and the d_{xz}/d_{yz} degeneracy is split. Here the most obvious effect of the ligands is to dramatically raise the energy of the Mn a_{1g} (d_{z^2})-orbital, owing to the repulsive interaction between the ligand HOMO and the metal d_{z^2}. As shown in Table 2, the oxidation and reduction patterns of $MnP/Pc(py)_2$ are similar to those of MnP/Pc. An exception is the second oxidation of $MnP(py)_2$, which occurs at the central metal to yield a $[Mn^{IV}P(py)_2]^{2+}$ species, different from the situation with MnP. On the other hand, the second oxidation of $MnPc(py)_2$ may occur either at the metal or at the Pc ring since the respectively resulting $^4B_{2u}$ and $^4B_{1g}$ states are nearly degenerate. As mentioned in the Introduction, there is some ambiguity about the nature of the first reduced product $[MnPc(py)_2]^-$. The calculation does not corroborate the argument[17] that the first reduction stage involves the addition of an electron to the Pc ring. Rather, the calculated result is consistent with the ESR measurement[17] which indicates a closed-shell anion.

The calculated properties of $MnP/Pc(py)_2$ in the ground state are collected in Table 5, together with the corresponding data of MnP/Pc for comparison. While it is shown that the Mn$-$N(eq) bond length in $MnP/Pc(py)_2$ is 0.01$-$0.02 Å longer than that in MnP/Pc, for the same $(d_{xy})^1(d_\pi)^4$ state the difference of the bond length between ligated and unligated complexes is less than 0.01 Å, which indicates minimal structural change in the equatorial plane upon addition of two axial ligands. The first IP of $MnP/Pc(py)_2$ is decreased by 0.4/0.3 eV as compared to that of MnP/Pc, suggesting that the axial ligation eases the oxidation. This ligation also decreases the electron affinity of the molecule, by 0.5/0.7 eV. The E_{bind} entry in Table 5 indicates that the two py ligands are bound to MnP by some 1.1 eV. The axial binding is stronger in $MnPc(py)_2$, where E_{bind} is 1.33 eV. We also evaluated the dissociation energy (E_{diss}) for $MnP/Pc(py)_2$ $\rightarrow$ MnP/Pc(py) + py, as it is reported that MnPor has the preference of adding only one ligand to form a five-coordinate complex.[7] Indeed, the calculated E_{diss} value is notably smaller for the porphyrin than for the phthalocyanine, which is in qualitative agreement with the experimental observation.

3.3.2. MnP(py) and MnPc(py). When only a single axial ligand is attached to the system, significant out-of-plane displacement of the metal is expected and, in fact, observed. The structural parameters of particular interest for these five-coordinate complexes are the Ct$\cdots$N(eq) distance (which

Table 6. Calculated Relative Energies (E) and Structural Parameters (R) for Different Configurations in MnP(py) and MnPc(py)

configuration									
$1a_{1g}/d_{xy}$	$1b_{3g}/d_{yz}$	$1b_{2g}/d_{xz}$	$2a_{1g}/d_{z^2}$	$b_{1g}/d_{x^2-y^2}$	state[a]	E (eV)	$R_{Ct\cdots Mn}$ (Å)	$R_{Ct\cdots N(eq)}$ (Å)	$R_{Mn-N(ax)}$ (Å)
					(a) $MnP(py)_2$				
1	1	2	1	0	$^4B_2$ (^4E_g)	0.05	0.132	1.997	2.220
2	1	1	1	0	$^4A_2$ ($^4A_{2g}$)	0.39	0.173	1.996	2.233
1	1	1	1	1	$^6A_1$ ($^6A_{1g}$)	0	0.424	2.042	2.210
1	2	2	0	0	$^2A_1$ ($^2B_{2g}$)	0.27	0.158	1.996	1.930
2	1	2	0	0	$^2B_2$ (^2E_g)	0.40	0.200	1.991	1.919
					(b) MnPc(py)				
1	1	2	1	0	$^4B_2$ (^4E_g)	0	0.151	1.938	2.219
2	1	1	1	0	$^4A_2$ ($^4A_{2g}$)	0.47	0.196	1.942	2.222
1	1	1	1	1	$^6A_1$ ($^6A_{1g}$)	0.55	0.427	1.956	2.115
1	2	2	0	0	$^2A_1$ ($^2B_{2g}$)	0.16	0.134	1.942	1.931
2	1	2	0	0	$^2B_2$ (^2E_g)	0.41	0.165	1.946	1.926

[a] States in parentheses are the corresponding states in unligated MnP/Pc.

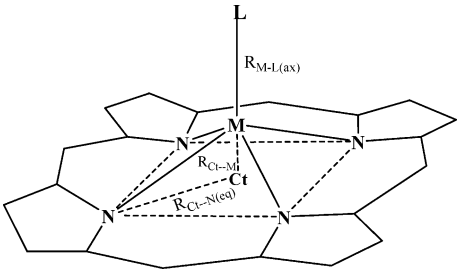

Figure 4. Coordination group for five-coordinate metal porphine MP(L). $R_{Ct\cdots N(eq)}$ denotes the distance between the center of the ring (Ct) and the equatorial nitrogen atom [N(eq)], $R_{Ct\cdots M}$ denotes the distance between Ct and M, and $R_{M-L(ax)}$ denotes the distance between M and the axial ligand L.

indicates the ring core size), Ct···M distance (which indicates the metal, M, out-of-plane displacement), and axial M−L(ax) bond length; they are illustrated in Figure 4. As was done above, the energetics of possible low-lying states were computed and geometry optimization was carried out for each state. The results are collected in Table 6.

3.3.2.a. MnP(py). MnP(py) is calculated to be high spin, in agreement with experimental observation.[7] Figure 3 shows the changes of the valence MOs when one py is removed from $MnP(py)_2$. The d_{z^2}- and $d_{x^2-y^2}$-orbitals, which are empty in $MnP(py)_2$, are lowered enough to be occupied in MnP(py). In addition to $R_{Ct\cdots N(eq)}$, the out-of-plane Ct···Mn distance depends on the spin multiplicity as well: it is 0.13−0.17 Å for the low- and intermediate-spin states and 0.42 Å for the high-spin state. For a given state, $R_{Ct\cdots N(eq)}$ in MnP(py) is very close to $R_{Mn-N(eq)}$ in MnP, again indicating that the size of the porphyrin core is not affected much by interactions with the axial ligand. Compared to that in $MnP(py)_2$, the axial Mn−N(ax) distance in MnP(py) is significantly shortened, especially for the states with an electron in the d_{z^2}-orbital. No X-ray crystal structure data are available for MnPor(py).

3.3.2.b. MnPc(py). In contrast to P, the Pc ring, with a smaller core size, gives rise to an intermediate-spin MnPc(py) complex, where the d_{z^2}-orbital is occupied but $d_{x^2-y^2}$ is empty. Thus MnPc(py) has a $^4B_2$ (^4E_g) ground state, similar to MnPc. The high-spin $^6A_1$ ($^6A_{1g}$) state lies about 0.6 eV higher in energy (1.09 eV for MnPc). Except the difference in the ground state, some conclusions drawn above for MnP(py) also apply to MnPc(py). So far, no observation of the MnPc(py) species has been reported in the literature (to our knowledge). For MnPc in solution, it is common for Mn^{II} to attach axially to two solvent molecules.[6,17,18] The calculated binding energy between MnPc and py is 0.51 eV, comparable to that of MnP−py (0.52 eV in the ground state). But the MnPc−$(py)_2$ binding energy is significantly larger than that of MnP−$(py)_2$.

4. Summary

By calculating the energetics of a number of possible low-lying states, the ground-state configuration of each system considered here was determined. While MnTPP in the crystal structure is high spin ($S = {}^5/_2$) with the Mn^{II} atom out of the porphyrin plane, the free MnP molecule has no obvious tendency to distort from planarity even in the high-spin state. The ground state of the planar structure is an intermediate-spin ($S = {}^3/_2$) state, as previous EHMO calculations suggested.[2] Since the present DFT method probably overestimates the energy of the high-spin state, the calculated ground state for MnP is subject to verification through experimental (magnetic or ESR) studies of the gas-phase species. It is possible that the high-spin state of MnTPP in the crystal is induced by significant intermolecular interactions which effectively change the coordination number of the metal and also draw the metal out of the porphyrin plane.

The free MnPc molecule is calculated to have a ^4E_g ground state arising from the $(d_{xy})^1(d_\pi)^3(d_{z^2})^1$ configuration, in agreement with the more recent MCD and UV−vis measurements of MnPc in an argon matrix[14] but different from the early magnetic measurements of crystal MnPc which yielded a $^4A_{2g}$ ground state arising from the $(d_{xy})^2(d_\pi)^2(d_{z^2})^1$ configuration.[13] The fact that there are N atoms of adjacent parallel molecules lying ∼3.2 Å above and below the metal atom was suggested to be the reason for a $^4A_{2g}$ ground state in the crystal.[14,15] A calculation on a model system MnPc···$(HCN)_2$ shows that the weak axial ligation indeed lowers the relative energy of $^4A_{2g}$ notably but is not able to change the energy order between the ^4E_g and $^4A_{2g}$ states. Other intermolecular effects may also need to be considered in order to account for the ground state of solid MnPc. The first oxidation of MnPc occurs at the central metal, in contrast to the macro-ring oxidation in the FePc analogy. The electronic properties of MnPc differ somewhat from those

of MnP due to the presence of benzo groups and shorter Mn−N(eq) bond lengths in the former molecule.

Upon complexation of two axial py ligands to MnP/Pc, the Mn^{II} ion becomes low spin ($S = {}^1/_2$), having a ground-state configuration of $(d_{xy})^1(d_\pi)$.[4] The calculated geometry parameters in $MnPc(py)_2$ at this low-spin state are in good agreement with the X-ray crystal structure data. The recent assignment of this complex as an intermediate-spin $(d_{xy})^2(d_\pi)^2(d_{z^2})^1$ ground state[16] is questionable. As a ligand with strong σ-donor but weak π-back-bonding ability, py raises the Mn d-orbital energy levels. Thus the one-electron oxidation of $MnP/Pc(py)_2$ occurs at the metal as in unligated MnP/Pc, and the ionization potentials are reduced relative to the case of MnP/Pc. The $[MnP/Pc(py)_2]^-$ ion results from the addition of an electron to a d-orbital of the metal, and so it is a closed-shell system. This result is consistent with the ESR measurement[17] and against the argument[17] that the first reduced product of $MnPc(py)_2$ involves reduction of the Pc ring.

When one py is removed from $MnP/Pc(py)_2$, the other py then "pulls" the metal out of the plane toward itself in order to avoid strong repulsion forces with the P/Pc nitrogen atoms. In this case the Mn $d_{x^2-y^2}$- and d_{z^2}-orbital energy levels are lowered significantly. For MnP, the $d_{x^2-y^2}$-orbital is lowered enough to be occupied, and so this five-coordinate molecule becomes high spin. But the smaller core size of Pc results in less lowering of the $d_{x^2-y^2}$ energy level, and so MnPc(py) is an intermediate-spin system. While the MnP−py bond strength [in MnP(py)] is comparable to that of MnPc−py, the MnP−$(py)_2$ binding energy is notably smaller than that of MnPc−$(py)_2$. This may be one of the reasons why, in solution, MnPc picks up two solvent molecules (L) to form a six-coordinate $MnPc(L)_2$ complex, while five-coordination of Mn^{II} prevails for manganese porphyrins.

Acknowledgment. This work was supported by the National Institutes of Health (S06 GM08047). The authors gratefully acknowledge the computational facilities provided by the Mississippi Supercomputer Center.

Supporting Information Available: ADF calculations on iron porphine (FeP) and a comparison of the results from different computational methods; comparison among Mn^{II}, Fe^{II}, and Co^{II} complexes. This material is available free of charge via the Internet at http://pubs.acs.org.

IC0401039